Journal of Food Engineering 403 (2026) 112710

Contents lists available at ScienceDirect

Journal of Food Engineering

journal homepage: www.elsevier.com/locate/jfoodeng

Pickering water-in-oil emulsions stabilized by beeswax crystals: Design and stability

Yanhui Zhang [a,b], Elizabeth Tenorio-Garcia [b], Yanxiang Gao [a], Fanny Nascimento Costa [c], Michael Rappolt [b], Like Mao [a,***], Sepideh Khodaparast [d,**], Anwesha Sarkar [b,*]

[a] College of Food Science and Nutritional Engineering, China Agricultural University, Beijing, 100083, China
[b] Food Colloids and Bioprocessing Group, School of Food Science and Nutrition, University of Leeds, LS2 9JT, Leeds, UK
[c] The Bragg Centre for Materials Research, University of Leeds, LS2 9JT, Leeds, UK
[d] School of Mechanical Engineering, University of Leeds, LS2 9JT, Leeds, UK

ARTICLE INFO

Keywords:
Pickering particles
Oleogels
Beeswax
Contact angle
Emulsions
SEM

ABSTRACT

The aim of this study was to understand how beeswax can be used to stabilize water-in-oil emulsions and examine the impact of droplet volume fraction on emulsion stability. Pickering water-in-oil (W/O) emulsions were successfully designed using beeswax oleogels (4 wt%) as the sole stabilizer via a facile homogenization approach. The effects of beeswax crystals on the formation, stability, and structural organization of W/O emulsions (containing up to 70 % v/v water) were systematically investigated. Oleogelation reduced the interfacial tension between oil and water from 21 ± 1 mN/m to 14 ± 1 mN/m, enabling beeswax crystals to stabilize emulsions without the need for any synthetic surfactant. X-ray diffraction analysis revealed that beeswax crystals in oleogels exhibited a stable β' polymorph with orthorhombic packing, maintaining a reduced long-chain spacing from 7.8 nm in pure beeswax to 6.3 nm, which contributed to the stabilization of Pickering W/O emulsions. The emulsions ranged in size (D_{32}) from 8 to 16 μm depending upon the droplet volume fraction and showed no significant change over storage period of 6 weeks. Microscopic observations of the interface demonstrated that emulsion stability was achieved through the synergistic effects of both the Pickering stabilization and bulk network stabilization. This dual stabilization mechanism was further confirmed by thermal cycling experiments and *in situ* crystallization analysis at the interface as well as rheological measurements showing gel formation at higher volume fractions of droplets. Overall, these findings highlight the potential of beeswax to stabilize W/O emulsions for applications in food and allied soft matter industries.

1. Introduction

Pickering emulsions, in which droplets are covered by a layer of solid particles, have attracted a great deal of attention due to their enhanced stability and potential applications in food, pharmaceuticals, lipid-based active ingredient delivery, and personal care formulations (Cheng et al., 2024; Sarkar and Dickinson, 2020; Sarkar et al., 2019; Tenorio-Garcia, Araiza-Calahorra, Rappolt, Simone and Sarkar, 2023). In these systems, Pickering particles are irreversibly adsorbed at the liquid-liquid interface, forming an effective steric and often electrostatic barrier that prevents coalescence, and macroscopic phase separation (Koroleva and Yurtov, 2022). While some functional particles inherently exhibit the interfacial properties required for stabilizing Pickering water-in-oil (W/O) emulsions, others may have a strong affinity for either the oil or water phase, resulting in limited interfacial adsorption and reduced emulsion stability (Kim et al., 2025). Traditionally, oil-soluble surfactants such as polyglycerol polyricinoleate (PGPR), Span80, glycerol monooleate, and some nanoparticles such as hydrophobic silica (SiO_2), titania (TiO_2), and carbon nanotubes (CNTs) with static water contact angles above 90° have been used to stabilize W/O emulsions (Hong et al., 2023). However, concerns over their environmental impacts and sustainability have driven the search for naturally derived, food-grade particles with interfacial stabilizing properties.

Recent investigations have identified oleogels prepared using

* Corresponding author.
** Corresponding author.
*** Corresponding author.
E-mail addresses: likemao@cau.edu.cn (L. Mao), s.khodaparast@leeds.ac.uk (S. Khodaparast), A.Sarkar@leeds.ac.uk (A. Sarkar).

https://doi.org/10.1016/j.jfoodeng.2025.112710
Received 7 March 2025; Received in revised form 22 June 2025; Accepted 23 June 2025
Available online 24 June 2025

naturally sourced organic crystals such as cocoa butter fat, shellac, β-sitosterol and γ-oryzanol as a promising candidate for the preparation of stable W/O emulsions (Huang et al., 2023; Septiyanti et al., 2021; Tenorio-Garcia et al., 2023). Oleogels, are semi-solid systems in which the liquid oil is trapped by oleogelators to form a self-supporting structure, which can then provide a network to effectively stabilize water droplets (Zhang et al., 2023). Oleogelators can be either high- or low-molecular-weight compounds, among which waxes are promising alternatives thanks to their availability, renewability, biocompatibility, and inherent hydrophobic properties (Merchan Sandoval, Carelli, Palla and Baumler, 2020). Oleogel-based emulsions generally function by modifying the bulk rheological properties of the oil phase, forming a viscoelastic gel network that helps to maintain water droplet dispersion (Tenorio-Garcia et al., 2023). Among them, beeswax (BW) has been particularly recognized as a promising oleogelator due to its complex crystalline structure and GRAS status, making it widely applicable in food and pharmaceutical emulsions (Schaeffer et al., 2024). Previous research has shown that beeswax can significantly alter the viscoelastic properties of oleogels, contributing to overall emulsion stability through bulk structuring effects (Penagos et al., 2023). However, these studies have not systematically investigated whether beeswax crystals can also function as Pickering stabilizers at the oil-water interface.

Several recent studies have reported the formation of W/O emulsions by dispersing water in pre-formed oleogels, stabilizing droplets without additional surfactants (Du et al., 2025; Tenorio-Garcia et al., 2023). In some cases, wax crystals have been observed at the oil-water interface, hinting at a possible Pickering stabilization mechanism (Du et al., 2025). Notably, previous studies using plant-derived waxes (e.g., shellac wax, phytosterol crystal) have suggested that the presence of interfacial active crystals may contribute to emulsion stability (Song et al., 2025). However, these studies either did not explicitly analyze the Pickering stabilization mechanism or relied on indirect evidence, leaving the fundamental stabilization mechanism largely unresolved. Additionally, most existing work has relied on thermal melting methods, where waxes are first dissolved at high temperatures before emulsification. While effective, these methods pose several challenges: (i) high energy consumption, (ii) potential degradation of heat-sensitive compounds, and (iii) limited control over crystallization kinetics during cooling, which may affect emulsion stability (Jia and Zhang, 2024).

Motivated by these gaps, here we trial a room-temperature approach to construct stable W/O emulsion with high water content stabilized solely by beeswax crystals. Systematic tests, including multiscale microstructural observation, X-Ray diffraction, *in situ* crystallization analysis at the interface, and particle size analysis were carried out. We aimed to examine the behavior of beeswax crystals and to explain the stabilization mechanism of this surfactant-free emulsion. The findings provide new insights into the physicochemical basis of beeswax-stabilized emulsions, offering a sustainable alternative to conventional surfactants and expanding the application of natural wax-based emulsifiers in food, personal care, and other soft material formulations.

2. Materials and methods

2.1. Materials

Refined beeswax (BW) was purchased from Aromantic.co.uk. The main components have been reported to be linear monoesters and hydroxy monoesters, 35–45 %; complex esters, diesters, and triesters, 15–27 %; odd-numbered straight-chain hydrocarbons, 15 %; free fatty acids, 12–14 %; and free fatty alcohols, 1 % (Tulloch, 1971). Corn oil (CO) was obtained from KTC Edibles Ltd (UK). Nile blue and Nile red dyes were bought from Sigma Aldrich (St. Louis, MO, USA).

2.2. Preparation of oleogels

Oleogels were prepared using a combination of BW and CO by subjecting the mixture to a controlled crystallization process. First, 2, 4, and 6 wt% BW was mixed with CO at 80 °C using a stirrer on a hot plate for at least 30 min to ensure all the wax crystals were melted and soluble in the oil (Sarkisyan et al., 2023). Subsequently, the mixture was added to a jacketed vessel connected to a Huber Ministat 230 thermostat (Germany) to ensure crystallization at a controlled temperature. The jacket temperature was reduced from 75 to 25 at 2 °C/min cooling rate and maintained at 25 °C for 4 h. During the crystallization process, the samples were continuously sheared at 200 rpm using an overhead electric stirrer while the temperature was continuously monitored using a PT-100 temperature sensor inside the vessel. Light absorbance and transmittance were measured by a Control 4000 turbidimeter device (Optek, Germany) equipped with an ASD12-N absorption probe. The oleogels obtained in vessel were maintained at 25 °C before emulsion preparation. The resulting oleogels were named BW2, BW4, and BW6 containing 2, 4 and 6 wt% beeswax in the final samples.

2.3. X-ray diffraction (XRD)

Crystal structures were analyzed by X-ray diffraction (XRD), using a Bruker D8 diffractometer with monochromatic Cu Kα radiation (2θ range 2°–70°, step size = 0.03°). Measurements were performed for BW, CO, and oleogels containing different concentrations of beeswax, namely 5, 10, 20, 40, 60 and 80 wt%. The XRD data for BW was also captured during heating and cooling cycles between 25 °C and 80 °C. Temperature was increased/decreased in 5 °C steps and samples were held for 5 min at every temperature to ensure stabilization.

2.4. Interfacial tension and wettability measurements

Interfacial tensions of corn oil and oleogels were determined based on the optical pendant drop technique using a tensiometer setup (Theta, Biolin Scientific) in shadow-graphy mode. Oleogels of 0.5 wt% BW were tested as higher concentrations reduced the transparency and increased the viscosity of the solutions with adverse impacts on the reliability of the optical measurements. The wettabiliity of the oleogels was evaluated by water contact angle measurements. Static contact angle measurements were performed at 20 °C using a customized drop-shape tensiometer fitted with a tube microscope lens and DSLR Nikon camera. Oleogels containing varying concentrations of beeswax (2, 4, 6, 8, 10, 20, 40, 60, and 80 wt%) were melted and subsequently coated onto glass slides, where they were cooled to form smooth surfaces. Static contact angles were measured using the sessile drop method. Water droplets (3 μL) were produced using a straight needle of 0.52 mm outer diameter and 0.26 mm internal diameter onto the surface of the solidified oleogel. The droplet contour was fitted using the drop shape analyzer plugin of ImageJ software, and the contact angles between the oleogel and the water droplet were measured by averaging the right and left contact angles.

2.5. Preparation of W/O emulsions

The emulsions were prepared by mixing BW oleogels (BW4, 4 wt% beeswax in the corn oil) and the Milli Q water (10–70 % v/v), followed by homogenization with a high-speed blender (Ultra-Turrax S25N-18G, IKA, Staufen) at 12,000 rpm for 300 s. After the preparation, all samples were stored at 25 °C.

2.6. Microstructure of oleogels and W/O emulsions

Cryogenic Scanning Electron Microscopy (Cryo-SEM): A Helios G4 CX DualBean scanning electron microscope (FEI, USA) coupled with a PP3010T Cryo-FIG/SEM preparation system (Quorum Technologies, UK) was used to obtain morphology of the oleogel (BW4), and W/O emulsions (20–60 % v/v water). The sample was placed into a prechilled rivet holder and rapidly frozen using liquid nitrogen. Subsequently, the

sample was positioned in the sample preparation chamber, maintained at a temperature of −145 °C in a vacuum environment with a pressure of less than 10^{-7} mbar. It was then cleaved using a chilled, sharp blade and subjected to sublimation at −90 °C. Finally, the sample was re-cooled to −145 °C, coated with iridium via sputtering at a current of 10 mA for 30 s and moved into the microscope chamber. The imaging process was conducted at an accelerating voltage of 2 kV and a beam current of 0.10 nA.

Cross-polarized Light Microscopy (PLM): Cross-polarized imaging was performed using an Olympus BX53M optical microscope (OM) equipped with a Peltier device (Linkham PE120) for temperature control. A 20X long-working distance (Olympus LMPLFLN 20X) and a digital CMOS camera (Basler ace acA2040-90uc) were used for imaging. The sample temperature was varied from 25 °C to 70 °C during heating and cooling cycles at a rate of 1 °C per minute. Images were captured every 20 s to record the changes in the sample during the heating and cooling cycles. To visualize the location of wax crystals in a simple oil-water system, water and oil droplets were placed adjacent to each other on the stage at 70 °C and covered with a cover slip to form an interface.

Confocal Laser Scanning Microscopy (CLSM): The microstructure of the emulsions was characterized using a Zeiss LSM 880 inverted microscope (Carl Zeiss MicroImaging GmbH, Jena, Germany). The dye solution consisted of Nile Red (diluted to 0.1 mg/mL in dimethyl sulfoxide) and Nile Blue (diluted to 0.1 mg/mL in Milli Q water). Before the test, 20 μL dye solution was mixed with 1 mL emulsion (Tenorio-Garcia et al., 2023). The stained emulsions were then transferred to a concave well of confocal microscope slides, covered with a glass slide, and allowed to settle for about 10 min before being examined under the microscope. Image acquisition was performed through an oil immersion 63× objective, with the pinhole adjusted to 1 Air Unit to minimize light scattering. For fluorescence excitation, a wavelength of 488 nm was set for Nile Red, and 625 nm for Nile blue.

2.7. Droplet size distribution

A Malvern MasterSizer 3000 (Malvern Instruments Ltd, Malvern, Worcestershire, UK) equipped with Hydro SM was used to measure the droplet size distribution of the emulsions. The relative refractive index of the oil phase and droplet was set as 1.456 and 1.330, respectively. The droplet size was collected as Sauter-average diameter (D_{32}).

$$D_{3,2} = \frac{n_i D_i^3}{n_i D_i^2}, \quad (1)$$

where n_i represented the count of droplets with diameter D_i.

2.8. Rheological measurement

The rheological properties of the samples were analyzed using an Anton Paar MCR 302 rheometer (Anton Paar Ltd., Austria) equipped with a temperature control unit and a stainless-steel parallel plate (50 mm diameter). The test gap was set to 1000 μm. The steady shear viscosity of the emulsions was measured over a shear rate range of 0.1–1000 s^{-1}. The linear viscoelastic region (LVR) was determined through a strain sweep (0.01–1000 %) at 25 °C and 1 Hz. A frequency sweep was conducted from 0.1 to 100 Hz at a strain of 0.02 % (within the LVR), and the evolution of G′ and G″ was recorded as a function of frequency. All the test was conducted at 25 °C.

2.9. Statistics

All experimental results are presented by the mean and standard deviation of at least three measurements on triplicate samples (n = 3 × 3). Origin Pro 2021 was used to analyze the test data and draw the plots. SPSS 20.0 was applied to analyze the variance (ANOVA) of data with a significant level of $p < 0.05$.

3. Results and discussion

3.1. Properties of beeswax-based oleogels

The oleogel is the critical building block of a stable emulsion, therefore, it is essential to examine the properties of the beeswax (BW) crystals and the corresponding oleogels formed at various beeswax concentrations. The apparent transparency of the oleogel solutions gradually decreased with increasing beeswax content, as shown in Fig. 1A. At a BW concentration of 4 wt%, the oleogel displayed a self-supporting structure, forming a semi-solid gel. In a broader context, the formation and structural organization of crystals in oleogels are significantly influenced by both the crystallization process and the BW concentration (Han et al., 2022). Thus, temperature was controlled and maintained the same avoiding any effect from thermal fluctuations. Fig. S1 illustrates the real time the crystallization process of oleogels containing 2, 4, and 6 wt% BW. Changes in light transmittance and absorbance values were used to detect the onset of crystals formation in the oil mixture. A sudden decrease in transmittance and the sharp increase in absorbance indicated the initiation of crystallization at the crystallization temperature (T_c) (Metilli et al., 2021; Tenorio-Garcia et al., 2023). As shown in Fig. S1A–C, BW6 exhibited the highest T_c (47.50 ± 0.44 °C), followed by BW4 (45.2 ± 0.11 °C) and BW2 (42.62 ± 0.39 °C), demonstrating that the T_c increased proportionally with BW concentration.The higher beeswax concentration provided additional nucleation sites, facilitating earlier crystallization. Consequently, the shear viscosity also increased with BW content due to the formation of a denser crystal network, leading to greater resistance to flow (Fig. S2).

Based on the gel-like texture (Fig. 1A) and results of the preliminary storage experiments (Fig. S3), the oleogel with 4 wt% beeswax (BW4) was selected for emulsion formulation due to its potential future industrial applications (Han et al., 2022). Fig. 1B and C depicted the crystal morphology of BW4 with PLM and cryo-SEM. In the PLM images, BW4 exhibited tightly packed needle-shaped crystals, which provided a robust physical network for structuring the liquid oil (Tavernier et al., 2017). This observation was further supported by the cryo-SEM image in Fig. 1C, which also revealed a needle-like crystal morphology (showed by the yellow arrows) capable of effectively trapping the oil phase.

Crystal structure of beeswax and oleogels. XRD was utilized to examine the structure of pure BW crystals and those within the oleogels. Fig. 2 and S4 show the diffraction patterns for BW100 and examples of oleogels at varied concentrations of BW. Small-angle diffraction peaks for BW100 presented in Fig. 2A show the long-spacing ordering of the crystals formed of long carbon chains, mainly attributed to the diesters and fatty acids in the wax (Gaillard et al., 2011). Further analysis of the small-angle peaks showed a reduction in the long chain spacing from 7.8 nm for BW100 to 6.3 nm for BW crystals in the oleogels (Fig. S5). These observed long-spacing values and respective chain tilt values of 0° and 36°, respectively, agree well with the reported stacking arrangements of diesters in beeswax. The average wax ester was estimated to be of approximately 60 carbon chain length in line with the previously reported values of C56-C64 for BW diesters (Schoening, 1980; Tulloch, 1971).

Fig. 2B demonstrates the wide-angle region, where two strong diffraction peaks are observable at q values 15.2 nm^{-1} and 16.9 nm^{-1}, corresponding to lateral packing of wax molecules with spacings of 4.12 Å and 3.71 Å, respectively. These two peaks indicate the β′ polymorph formed of orthorhombic packing of chains (Liu et al., 2019; Schoening, 1980). The scattering pattern of the corn oil exhibits only two broad diffuse lobes, corresponding to the characteristic spacings of 4.6 Å and 2.2 Å, which confirms the fluid state of the corn oil. Note, the average next nearest chain neighbour distance in the fluid state is about 4.6 Å. The main diffraction peaks of BW crystals were detectable in all oleogels with the peak intensities increasing with the concentration of the BW,

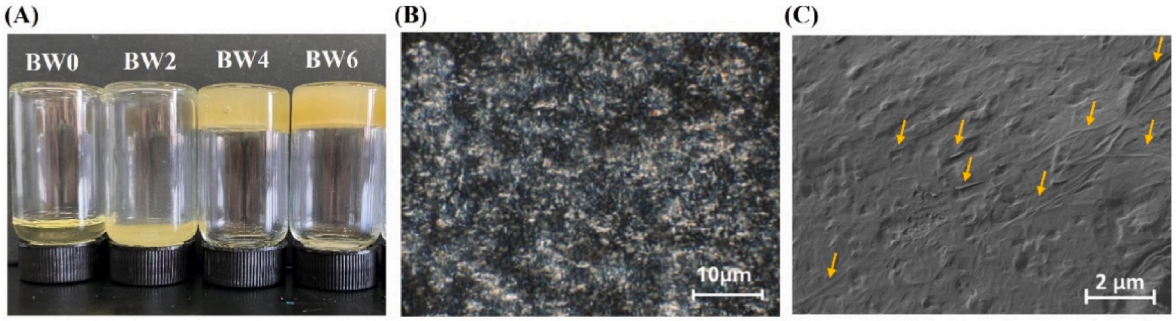

Fig. 1. **(A)** Images of beeswax oleogels (BW0: corn oil, BW2: 2 wt% beeswax in oleogel, BW4: 4 wt% beeswax in oleogel, BW6: 6 wt% beeswax in oleogel) in upside down vials showing the transparency and flowability of the solution. **(B)** Cross-polarized light micrograph and **(C)** cryo-scanning electron microscopy (cryo-SEM) images of BW4 oleogels. Yellow arrows point to the location of the crystals. (For interpretation of the references to colour in this figure legend, the reader is referred to the Web version of this article.)

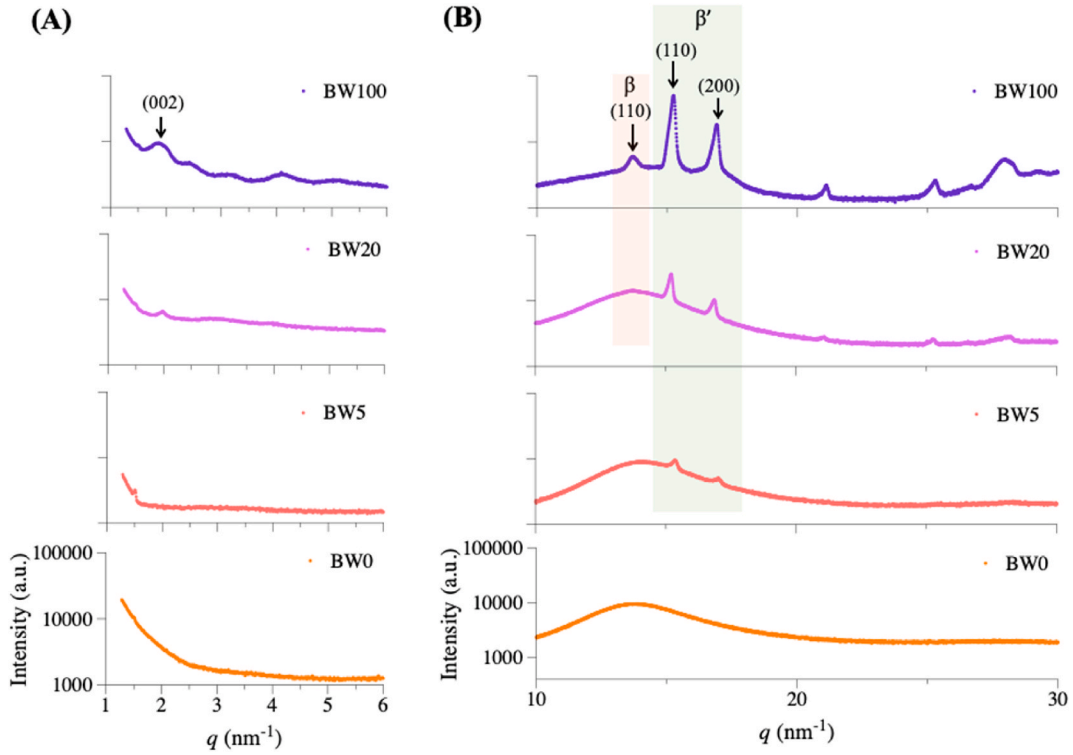

Fig. 2. X-ray diffraction (XRD) patterns of beeswax and oleogels containing different concentrations of beeswax (BW0: corn oil, BW5: 5 wt% beeswax in oleogel, BW20: 20 wt% beeswax in oleogel, BW100: pure beeswax). (**A**) Small-angle region showing peaks associated with the longitudinal packing of long-chain diesters. (**B**) Wide-angle region including two main peaks associated with the orthorhombic crystal structure of the β′ polymorph and a peak at smaller intensity attributed to the triclinic structure of the β polymorph. Indexing of other wide-angle peaks is presented in Fig. S4.

while the peak positions remained constant; see Fig. S4 for more BW concentrations. That is, the area per chain is with a value of 18.4 $Å^2$ conserved, when adding CO. We note, that the (110) and (200) reflections of the orthorhombic sub-cell reflects a four nearest neighbour arrangement of chains (Small, 1984). The β′ polymorph was maintained up to the BW melting point at above 60 °C (Fig. S6). The relatively weak peak at 13.7 nm^{-1} corresponding to 4.6 Å indicates the presence of a smaller amount of the β polymorph crystals with a triclinic chain packing structure. Further indexing of the wide-angle diffraction peaks for BW crystals was performed following the structure reported by Schoening (1980), see Fig. S4. XRD measurements at varied temperatures showed that the β polymorph is formed of wax components with relatively lower melting temperatures compared to the β' polymorph (Fig. S6) (Buchwald et al., 2008). This observation is in line with the two main endothermic peaks observed in differential scanning calorimetry (DSC) analysis of beeswax at temperatures 50–55 °C and 62–65 °C (Buchwald et al., 2008).

3.2. Formation of the W/O emulsions

3.2.1. Microstructure of the emulsions

BW crystals were found to exhibit outstanding potential for fabricating W/O emulsions with high water content, however, their stabilization mechanism has remained unresolved. Surfactant-free W/O emulsions with 30 % v/v water were successfully prepared by high-speed shearing at 25 °C, with microstructures shown in Fig. 3.

The droplets were fairly uniform in size and tightly packed with no coalescence events observed. The majority of water droplets in Fig. 3A1 appear non-circular, which is often a characteristic of Pickering emulsions (Ming et al., 2023). The distribution and arrangement of BW

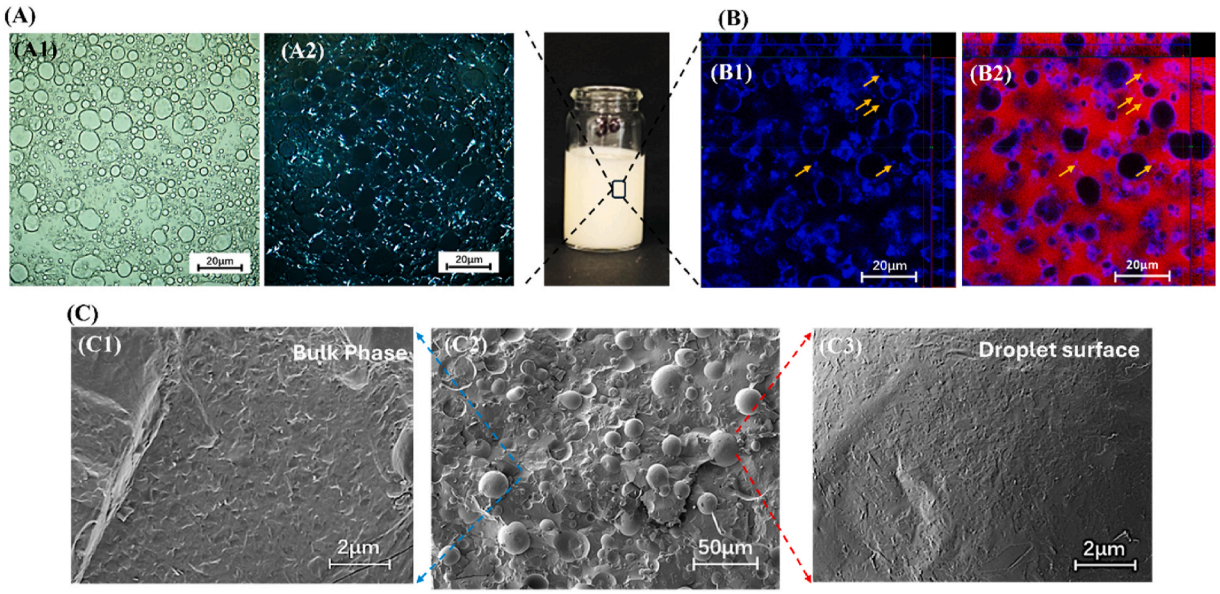

Fig. 3. Brightfield (**A1**), cross-polarized (**A2**), laser confocal (**B, B1**: crystals in emulsion, **B2**: crystals and oil phase in emulsion. Yellow arrows point to the location of the crystals in the bulk phase in the microscopy images of water-in-oil (W/O) emulsions (30 % v/v water) stabilized by oleogel (4 wt% beeswax in oleogel). The emulsions were fluorescently dyed with a blend of Nile Red and Nile Blue stains in B in order to differentiate the beeswax crystals from the bulk oil phase (corn oil), where Nile Blue preferentially stains the surface of beeswax crystals (blue) whilst Nile Red stains the bulk oil (red). Beeswax crystals at the interface of emulsions proved that the system was stabilized by Pickering crystals. Cryo-SEM image (**C**) of the 30 % v/v emulsion showing the bulk oil phase **(C1)**, the emulsion **(C2)** and interface of a droplet **(C3)**. (For interpretation of the references to colour in this figure legend, the reader is referred to the Web version of this article.)

crystals within the emulsion defines the stabilization mechanism, playing a crucial role in defining the final physical properties of the emulsion, which was initially examined using polarized light microscopy. The wax crystals were clearly noticeable at the water-oil interface of droplets under polarized light (Fig. 3A2), confirming their role in stabilizing the oil-water interface (Ghosh et al., 2011). The 3D confocal images in Fig. 3B further confirm the distribution of BW crystals at the water-oil interface. The interfacial tension of 0.5 wt% BW oleogel with water was measured to be 14 ± 1 mN/m, significantly smaller than the 21 ± 1 mN/m measured for the corn oil without any added wax (Fig. S7). This measurement further confirms the Pickering role of the wax crystals in reducing the overall energy of the W/O emulsion for a given number and size of water droplets (Dekker et al., 2023). Besides BW crystals at the interface, the fluorescent signal from the BW crystal particles was also captured in the continuous phase (arrows in Fig. 3B), indicating that the water droplets were additionally immobilized in the crystal network in the bulk (Chen et al., 2021). Similar behavior was found in other systems, where wax crystallization on the droplet interface provided stability against droplet coalescence while presence of crystals within the continuous phase reduced inter-droplet collisions (Gu et al., 2023). The dual role of BW crystals in stabilizing the W/O emulsion was also confirmed by the cryo-SEM images in Fig. 3C. As expected, a rough texture was found in the bulk phase, which has been reported to be the BW crystals in oil (Enamul Hossain et al., 2009; Wettlaufer et al., 2021). Interestingly, wax crystals are clearly detectable on the surface of the droplets as shown in the magnified images (Fig. 3C1) supporting the hypothesis of BW crystals acting as Pickering particles (Fig. 3C3). Additionally, some components in beeswax, such as free fatty acids and free fatty alcohols (e.g., oleic acid, stearic acid and tetracosanol), act as co-emulsifiers, working together with wax ester crystals to stabilize the interface (Shu et al., 2023; Zhang et al., 2021).

Above all, the crystal network in the bulk phase and the BW crystals at the interface hindered the migration of water droplets and improved the stability of water droplets within the continuous phase (Shi et al., 2024). The combination of the two effects resulted in highly stable W/O emulsions in line with those systems stabilized by paraffin wax (Chen et al., 2021).

3.2.2. *Thermal stability of the emulsions*

To further confirm the role of BW in stabilizing the droplets versus the bulk oil phase, crystallization and melting of BW crystals at the interface were characterized *in situ* during heating and cooling cycles. Fig. 4 shows the microstructure of the emulsions alongside XRD patterns of BW at varied temperatures.

The melting point of BW has been reported to be in the range of 60–65 °C with onset of melting observed from above 45 °C (Buchwald et al., 2008). During the heating process, the stabilizing BW crystals melted gradually leading to the total phase separation of water and oil at temperatures above 60 °C (Fig. 4A1-A3). Tracking the XRD peaks corresponding to the orthorhombic BW crystal structures in Fig. 4B clearly shows that significant crystal loss is only observed when temperature is raised above 50 °C, with no detectable peaks at temperatures above 60 °C. A significant number of water droplets were still detected at 60 °C possibly stabilized by smaller-sized BW crystals as confirmed by the XRD data in Fig. 4B. Heating the solution to 70 °C resulted in full melting of the BW crystals and coalescence of water droplets, see Fig. 4C. Cooling the mixture back to its original temperature resulted in crystal formation in the bulk oil and at the remaining oil-water interface reaching the maximum crystal content at temperatures below 40 °C as confirmed by the XRD data, Fig. 4D.

Crystallization of the BW within the oleogel in the vicinity of oil-water interface was further analyzed through *in situ* cross-polarized analysis demonstrated in Fig. 5. The oleogel was brought into contact with pure water at temperatures above the melting point of the BW to ensure the wax solubility, see an example micrograph of the interface between oleogel and water at 70 °C in Fig. 5A1 and A2. Upon cooling, the dissolved BW crystallized in the bulk oil phase (Fig. 5B1 and B2) and at the water interface at room temperature (Fig. 5C1 and C2) owing to the adsorption of surface-active compounds in BW (Moghtadaei et al., 2018). Location of the water-oil interface is depicted by arrows and dashed line in the full frame and zoomed-in images, respectively. Based on the above findings, we can confirm that the stabilization might be described as a "dual" mechanism (Pickering stabilization + network stabilization). Such *in situ* confirmation of crystallization of BW at the interface is reported for the first time in this work.

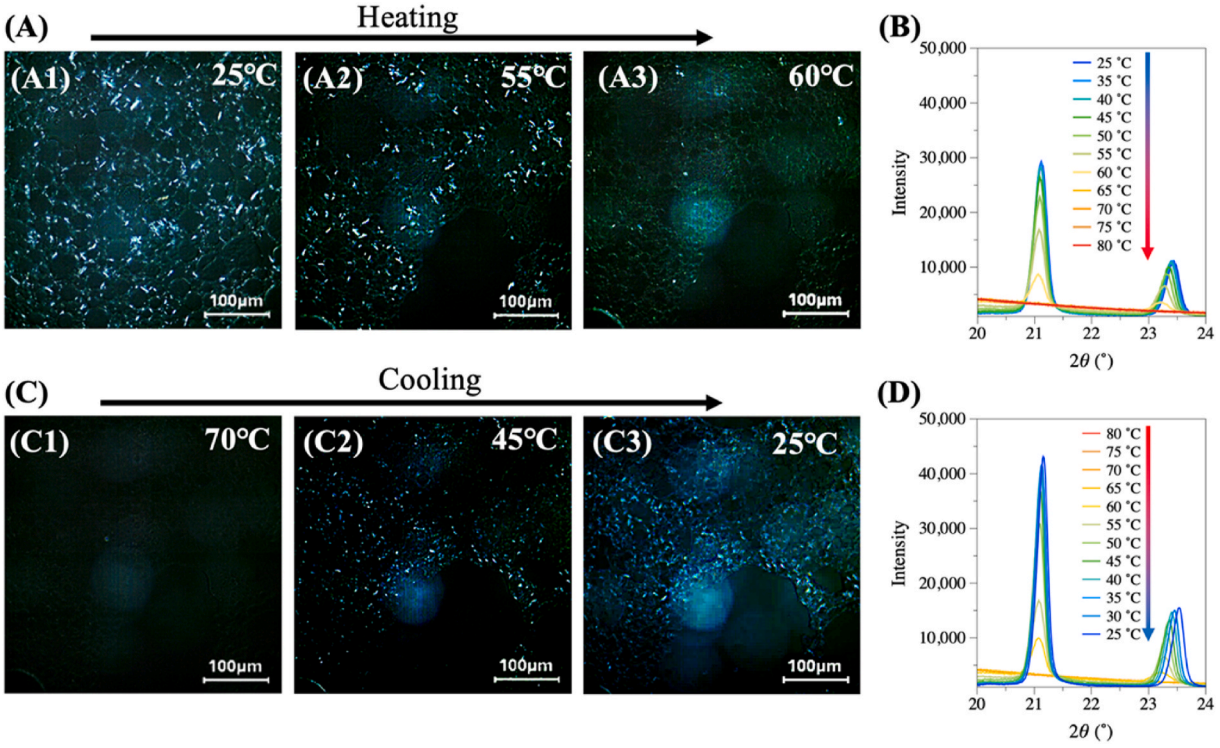

Fig. 4. Cross-polarized light micrographs (**A**: heating, **C**: cooling) and X-ray diffraction patterns (**B**: heating, **D**: cooling) of W/O emulsions (30 % v/v) during the heating and cooling process. The microstructure of the emulsions showed the changes as a function of temperature cycle which involved heating from 25 °C to 80 °C (**A1**: 25 °C, **A2**: 55 °C, **A3**: 60 °C) and cooling from 80 °C to 25 °C (**C1**: 25 °C, **C2**: 55 °C, **C3**: 60 °C). Stabilizing wax crystals were largely lost at temperature around 60 °C leading to droplet coalescence (A2 and A3). The XRD pattern shows a dramatic drop in the magnitude of the short-spacing peaks at 60 °C, while wax crystal structure was fully lost at 65 °C. Upon cooling the sample, the wax re-crystallized in the bulk and the remaining oil-water interface.

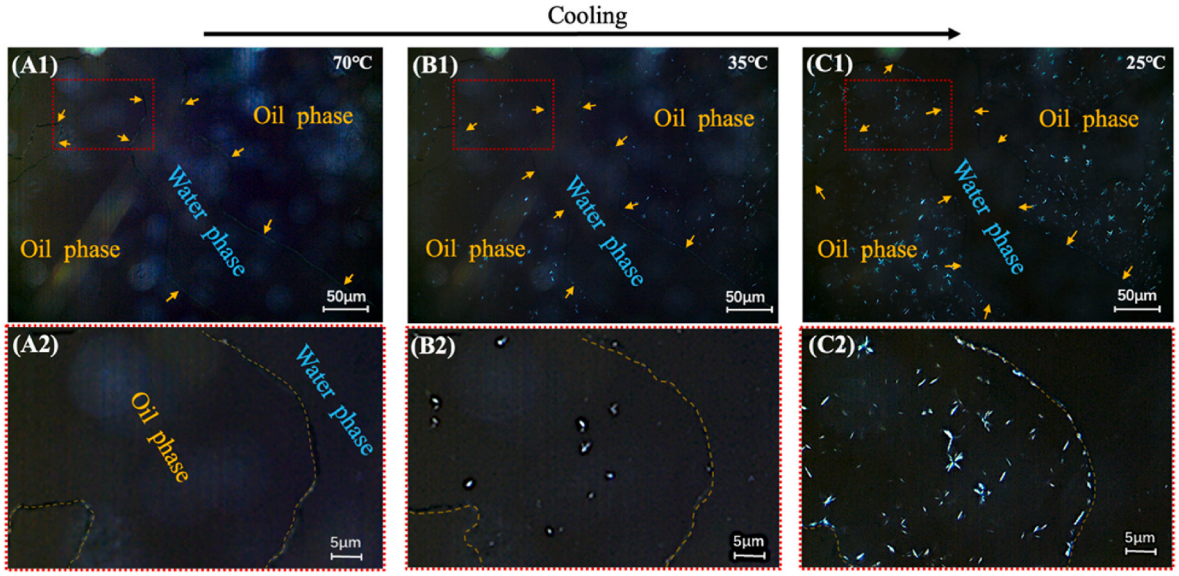

Fig. 5. Cross-polarized microscopy images of oleogel-water interface at different temperatures (**A**: 60 °C, **B**: 35 °C, **C**: 25 °C). Yellow arrows point to the location of the interface in A1, B1 and C1. Upon cooling the sample, wax crystals form in the bulk and at the oil-water interface. Close-up views of the region identified by the red dotted frame show the wax crystals in the bulk and at the interface highlighted by a dashed line during cooling (**A2**: 60 °C, **B2**: 35 °C, **C2**: 25 °C). (For interpretation of the references to colour in this figure legend, the reader is referred to the Web version of this article.)

3.3. Effect of water content on emulsion properties

3.3.1. Appearance and droplet size

Having confirmed the emulsion stabilization mechanism, we next investigated the maximum volume fraction of water in the W/O emulsions that can be effectively stabilized solely by BW crystals. To this end, emulsions with varying concentrations of water phase (10–70 % v/v) were successfully prepared through high-speed shearing, as shown macroscopically in Fig. 6A. All emulsions had a homogeneous appearance upon preparation, except for those with 70 % v/v water content, as

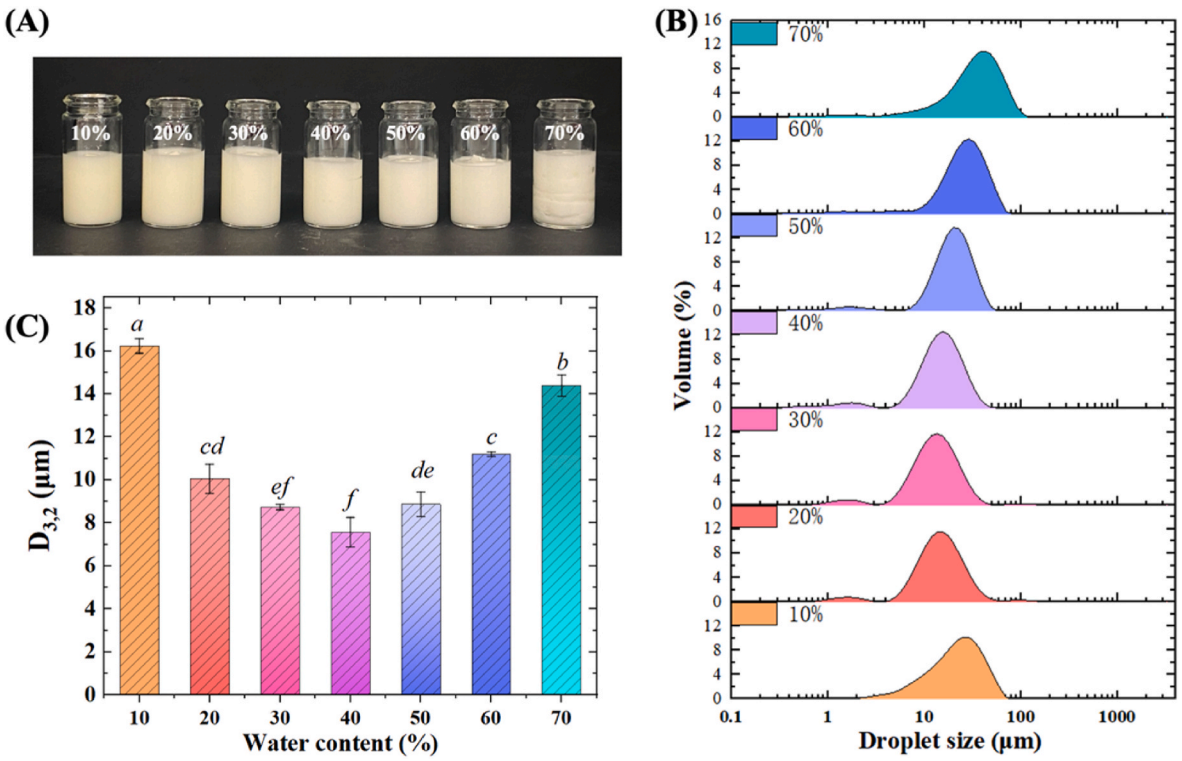

Fig. 6. Images of (**A**) the freshly prepared W/O emulsions containing different volume fractions of water (10–70 % v/v) showing kinetic stability. Droplet size distribution (**B**) and mean droplet size (**C**) of the freshly prepared emulsions containing various volume fractions of water (10–70 % v/v) stabilized by the beeswax crystals. Different lower-case letters in the bar plot in **C** indicate that the mean is statistically significant ($p < 0.05$). Mean and standard deviations are shown in C for a minimum of three measurements on triplicate samples (n = 3 × 3).

can be observed in Fig. 6A. The gel-like structures most likely resulted from the oleogelation of the continuous phase and the packing of the water droplets (Qiu et al., 2024; Zhang et al., 2021).

Droplet size is a key indicator for evaluating the stability and emulsification of the emulsions (Chondrou et al., 2024). Fig. 6B shows the droplet size distributions as a function of water content in the emulsion. Most droplet size distributions of W/O emulsions were bimodal. The distributions were skewed distribution curve to the left. Upon increasing the water content from 10 to 40 %, the mean droplet diameter decreased. Further increase in the water content resulted in a gradual shift in the distribution curve reflecting an increase in the droplet diameter. This behavior may be attributed to the unabsorbed BW crystals that aggregated in the bulk phase for relatively smaller water content (Öğütcü et al., 2015). At larger content, homogenization is expected to become more challenging resulting in higher packing of water droplet and overall larger mean diameters (Hong et al., 2022). A similar phenomenon was also observed by Gao et al. (2021) who reported that smaller droplet size for emulsions containing 25 and 40 % (v/v) water compared to those with 10 and 55 % (v/v) water content. Previous studies reported a maximum 55 % (v/v) water content for emulsions stabilized by beeswax-oleogel (Gao et al., 2021). The larger water content reported in our work is postulated to be attributed to the higher input energy of the emulsification process used here in comparison to the electromagnetic stirring proposed previously which did not provide enough energy to overcome the interfacial energy barrier between the two phases.

3.3.2. *Microstructure of emulsions*

CLSM images. The distribution of water droplets and BW crystals in the emulsions of increasing water content was visualized using CLSM (Fig. 7).

From the images in Fig. 7, we can observe that water droplets (in black) were dispersed in the oil phase (in red), while the BW crystals (in blue) were distributed at the interface and the bulk phase. It was revealed that the crystals were dispersed within the continuous phase and at the interface, stabilizing the emulsion by "wrapping" water droplets in a crystalline network. By comparing images of different volume fractions of water, it can be observed that droplets with regular shapes were sparsely distributed in the continuous phase in emulsions containing 20 % v/v water (Fig. 7A2). However, as the water content reached 60 % v/v, the droplets became more densely packed with relatively irregular shapes (Fig. 7C2). Such closely packed droplets are typically found in Pickering emulsions of larger dispersed phase volume (Lu et al., 2023; Zhao et al., 2019). Cryo-SEM analysis of the emulsions revealed the detailed structures of the emulsions (Fig. S8). In all the emulsions, the water droplets were encapsulated by the dense continuous phase of oil. The presence of BW crystals on the surface of the droplets suggested the formation of the Pickering emulsions (Fig. S8A), with additional dendritic crystals structuring the bulk phase (Fig. S8A). These observations provide additional support for the presence of a synergic interaction between the Pickering effect and network stabilization, which significantly enhances the emulsion stability.

3.3.3. *Rheological properties*

Fig. 8 presents the rheological properties of emulsions with varying water contents. The observed trends in viscosity (Fig. 8A), viscoelastic properties (Fig. 8B), and strain-dependent behavior (Fig. 8C) provide insights into the stabilization mechanisms governing these systems.

Fig. 8A presents the viscosity-shear rate relationship of emulsions. The emulsions exhibited shear-thinning behavior, where viscosity decreased with an increasing shear rate, indicating a non-Newtonian fluid characteristic. Higher water content resulted in increased viscosity, suggesting a stronger internal structure under low shear rate. At low water contents, the viscosity of the emulsions increased with higher water content (10–50 % v/v) across the entire shear range. This behavior was typical of systems where the gel network dominated

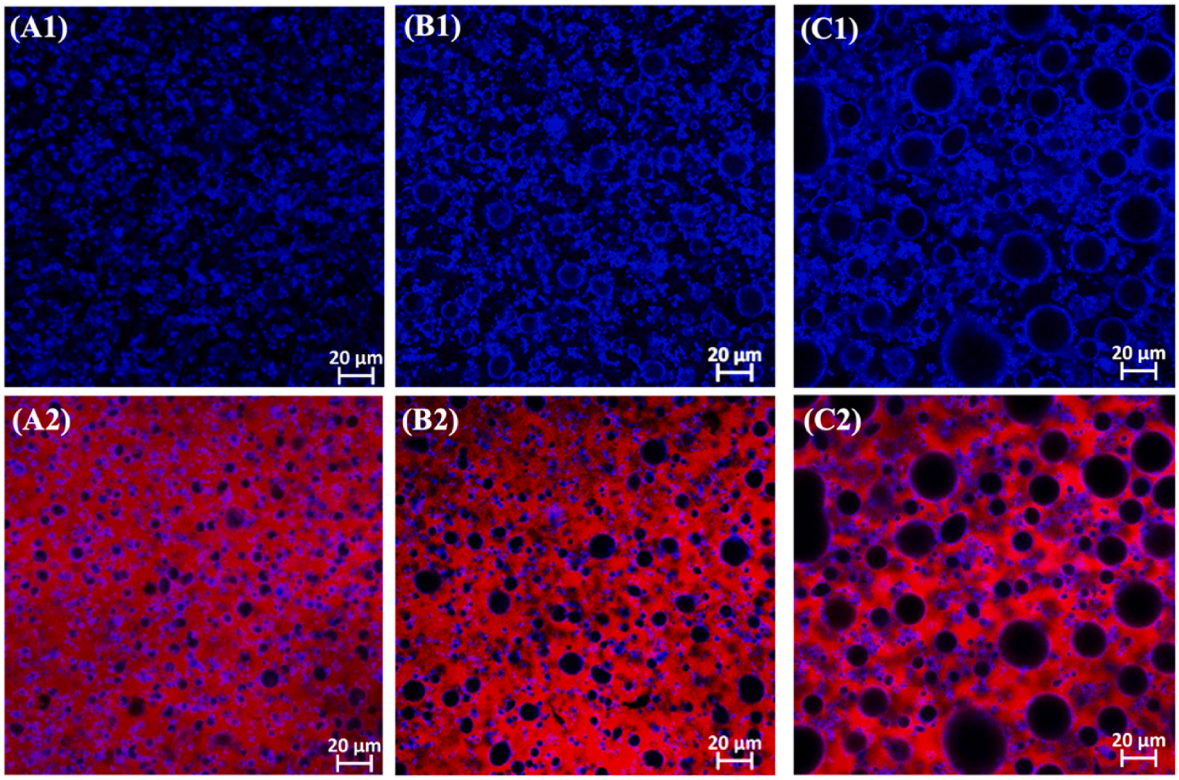

Fig. 7. Laser confocal micrographs of freshly prepared W/O emulsions containing different volume fractions of water (**A**: 20; **B**: 40; **C**: 60 % v/v). Beeswax crystals (**1**, blue) at the interface of freshly prepared W/O emulsions containing different volume fractions of water can be observed. The emulsions were fluorescently dyed with a blend of Nile Red and Nile Blue stains (**2**, red and blue) in order to differentiate the beeswax crystals from the bulk oil phase (corn oil), where Nile Blue preferentially stains the surface of beeswax crystals whilst Nile Red stains the bulk oil. (For interpretation of the references to colour in this figure legend, the reader is referred to the Web version of this article.)

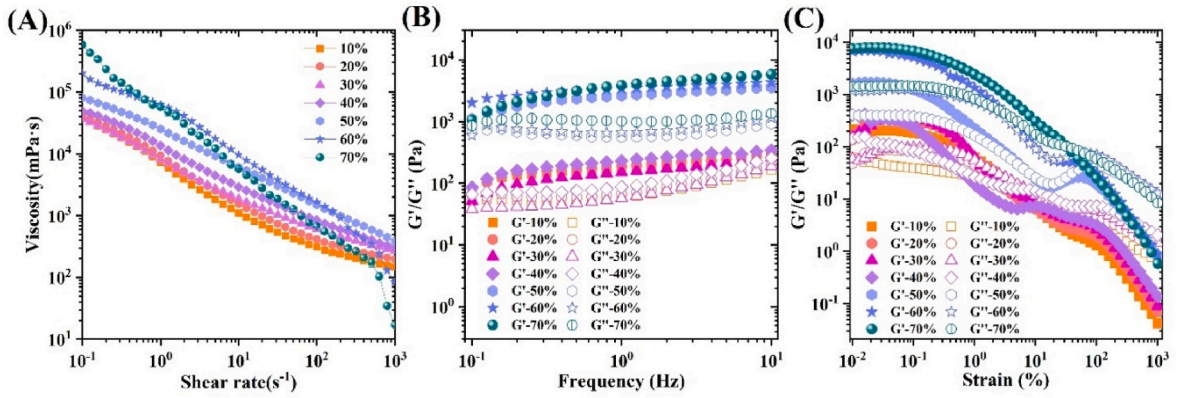

Fig. 8. Rheological properties of emulsions stabilized by BW4 with varying water contents (10–70 % v/v). (A) Shear test: the apparent viscosity as a function of shear rate. (B) Frequency sweep: storage modulus (G′) and loss modulus (G″) as a function of frequency. (C) Strain sweep: behavior of G′ and G".

(Wijarnprecha et al., 2021). On the other hand, a reduction in aqueous droplet size also contributed to the increase of emulsions' viscosity (Zhang et al., 2021). However, when the water content exceeded 50 %, shear thinning became particularly noticeable under high shear rates, especially in high-water-content systems. This suggested that the droplets moved along the shearing direction, indicating the dominance of the Pickering stabilization mechanism. Across all formulations in Fig. 8B, G' was higher than G", demonstrating the dominance of elastic behavior, characteristic of a gel-like structure (Han et al., 2024). As the water content increased from 10 % to 70 %, G′ progressively increased, with the 70 % water content emulsion exhibiting the highest G′ values over the entire frequency range. This indicated that a higher water content contributed to a stronger viscoelastic network, likely due to enhanced droplet interactions and structuring within the continuous phase. It is also proved that the water acted as active fillers in the system (Wijarnprecha et al., 2019). The increasing trend suggested that the emulsion stability was not solely dictated by the gel network of the oil phase but also influenced by the distribution and interaction between water droplets and the oil phase. Fig. 8C depicts the evolution of G′ and G''. All samples exhibited a linear viscoelastic region at low strains, followed by a sharp decrease in G′, indicating structural yielding (Zhang et al., 2023). The emulsion with 70 % water demonstrated the highest G′ value and highest yielded strain, confirming its superior structural resistance (Zhang et al., 2022). In contrast, lower water content

emulsions (10 %–40 %) exhibited lower moduli and yielded at lower strains, suggesting weaker internal networks. The results indicated that increasing the water content enhanced the structural integrity of the emulsions, likely due to the increased interactions between water droplets and the surrounding network. However, the role of the continuous phase gel network in stabilizing the system might have diminished at high water content, where Pickering-like stabilization effects became more dominant.

3.4. Storage stability

We observed that after 6 weeks of storage, all emulsions remained stable with no signs of coalescence and maintained their self-supporting gel-like structures, further demonstrating the macroscopic stability of the Pickering emulsions (Fig. 9A). The gel-like properties were largely due to the crystals in the bulk phase (oleogel). Size of water droplets was used as a quantitative indicator for evaluating the storage stability of emulsions. After 6 weeks of storage, the droplet size within the emulsions with different water content showed no significant change (Fig. 9B) (Geng et al., 2024). As can be seen from the right CLSM images (Fig. 9C), no significant coalescence of droplets was visible after storage for 6 weeks. Compared with the fresh images in Fig. 7, slight crystal aggregation was observed after long term as previously reported for BW particles by Jana and Martini (Jana and Martini, 2014). This, however, did not impact on the overall stability of the emulsions.

4. Conclusions

In summary, this study demonstrated that beeswax can effectively stabilize surfactant-free water-in-oil (W/O) emulsions through a combination of Pickering and network formation stabilization mechanisms. By simply mixing water and oleogels under high-speed shearing, we successfully prepared emulsions with up to 70 % v/v water content at less than 4 wt% of overall beeswax concentration without using any additional surfactant. The β' polymorph of beeswax, with its orthorhombic chain packing, was maintained in oleogels and emulsions, enhancing the stability of the Pickering water-in-oil emulsions. The crystallization behavior and polymorph stability of beeswax contribute significantly to the structural integrity of the emulsions. Optical microscopy analysis directly confirmed that beeswax crystals acted as Pickering particles stabilizing the interface of water droplets while providing structural stability to the oleogel. Beeswax crystals provided interfacial stability up to temperatures close to their melting point. Micron-sized droplets were characterized in all beeswax-stabilized emulsions with up to 70 % water. The viscoelastic properties of emulsions with varying water content demonstrated the dominance of beeswax-stabilized network enhancing emulsion structural integrity and stability in addition to the Pickerings stabilization. Furthermore, the emulsions displayed excellent storage stability, retaining similar droplet sizes and microstructures over several weeks of storage. Overall, these findings provide new insights into the stabilization mechanism of beeswax in W/O emulsions and offer valuable guidance for developing alternative surfactant-free emulsifiers. The water-in-oleogel systems introduced here could be used in future formulations to encapsulate hydrophilic and lipophilic nutrients for the formulation of drugs, cosmetics, food and other soft matter applications.

CRediT authorship contribution statement

Yanhui Zhang: Writing – review & editing, Writing – original draft, Methodology, Investigation, Formal analysis, Data curation, Conceptualization. **Elizabeth Tenorio-Garcia:** Writing – review & editing, Methodology, Data curation, Conceptualization. **Yanxiang Gao:** Writing – review & editing, Supervision. **Fanny Nascimento Costa:** Methodology, Investigation, Formal analysis. **Michael Rappolt:** Writing – review & editing. **Like Mao:** Writing – review & editing, Supervision. **Sepideh Khodaparast:** Writing – review & editing, Supervision, Methodology, Data curation, Conceptualization. **Anwesha Sarkar:** Writing – review & editing, Supervision, Project administration, Methodology, Conceptualization.

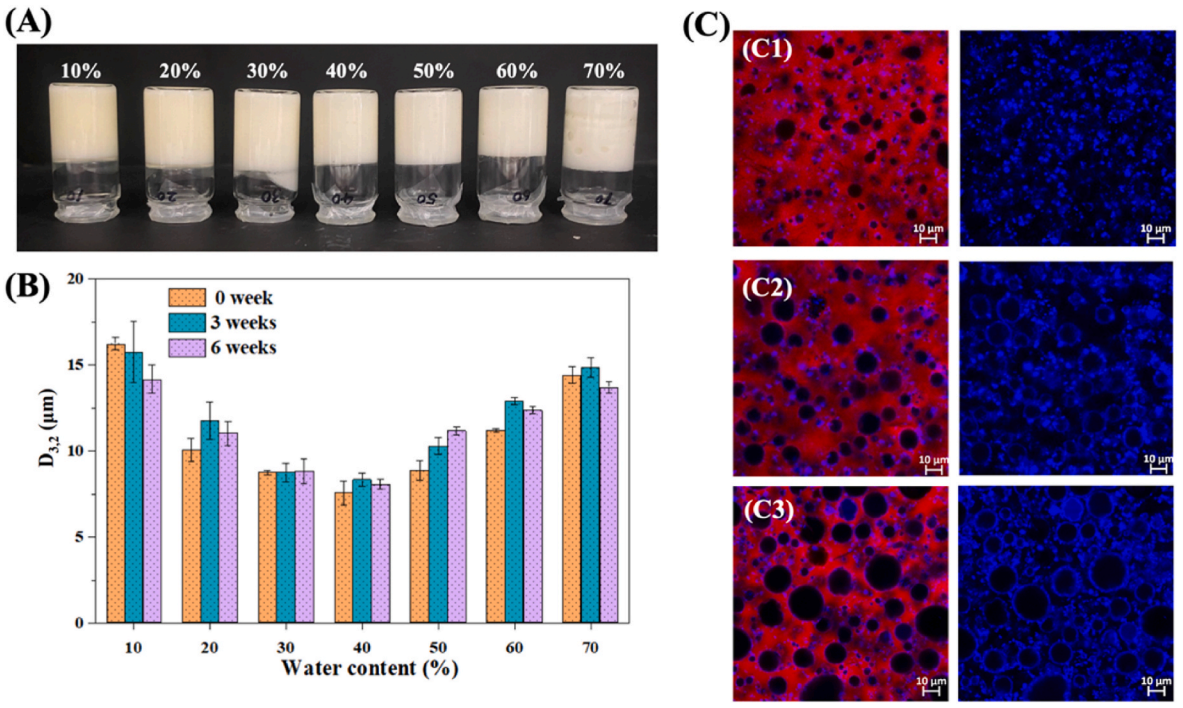

Fig. 9. Images of W/O emulsions at different volume fractions (**A**). Mean droplet size ($D_{3,2}$, μm) (**B**), and confocal micrographs (**C**, **C1**: 20 %, **C2**: 40 %, **C3**: 60 % v/v) of emulsions after 6 weeks of storage. The bottles containing the emulsions were put in an inverted position to highlight the solid-like behavior of the different samples. The droplet size of emulsions with different content of water showed no significant increase over 6 the weeks storage period ($p < 0.05$). Mean and standard deviations are shown in B for a minimum of three measurements on triplicate samples ($n = 3 \times 3$).

Declaration of competing interest

The authors declare that they have no known competing financial interests or personal relationships that could have appeared to influence the work reported in this paper.

Acknowledgements

This research was conducted at the University of Leeds funded by the China Scholarship Council (Grant No. 202306350104) and National Natural Science Foundation of China (No. 32272471).

Appendix A. Supplementary data

Supplementary data to this article can be found online at https://doi.org/10.1016/j.jfoodeng.2025.112710.

Data availability

Data will be made available on request.

References

Buchwald, R., Breed, M.D., Greenberg, A.R., 2008. The thermal properties of beeswaxes: unexpected findings. J. Exp. Biol. 211 (Pt 1), 121–127. https://doi.org/10.1242/jeb.007583.

Chen, X., Sun, G., Liu, D., Zhang, H., Zhang, H., Li, C., Zhao, Z., 2021. Two effects of wax crystals on stabilizing water-in-oil emulsions. Colloids Surf. A Physicochem. Eng. Asp. 625, 126884. https://doi.org/10.1016/j.colsurfa.2021.126884.

Cheng, Y., Cai, X., Zhang, X., Zhao, Y., Song, R., Xu, Y., Gao, H., 2024. Applications in Pickering emulsions of enhancing preservation properties: current trends and future prospects in active food packaging coatings and films. Trends Food Sci. Technol. 151, 104643. https://doi.org/10.1016/j.tifs.2024.104643.

Chondrou, A.P., Evgenidis, S.P., Karapantsios, T.D., Kostoglou, M., 2024. Emulsions stability in weightlessness: droplets size, droplets coalescence and phases spatial distribution. Colloids Surf. A Physicochem. Eng. Asp. 702, 134943. https://doi.org/10.1016/j.colsurfa.2024.134943.

Dekker, R.I., Velandia, S.F., Kibbelaar, H.V.M., Morcy, A., Sadtler, V., Roques-Carmes, T., Groenewold, J., Kegel, W.K., Velikov, K.P., Bonn, D., 2023. Is there a difference between surfactant-stabilised and pickering emulsions? Soft Matter 19 (10), 1941–1951. https://doi.org/10.1039/d2sm01375d.

Du, L., Guo, Y., Meng, Z., 2025. Organogels, O/W and W/O emulsion gels structured by monoglycerides: the study on the gelation behavior and crystal network. Eur. Food Res. Technol. 251 (2), 165–177. https://doi.org/10.1007/s00217-024-04613-w.

Enamul Hossain, M., Safiur Rahman, M., Islam, R., 2009. SEM-based Structural and Chemical Analysis of Paraffin Wax and Beeswax for Petroleum Applications.

Gaillard, Y., Mija, A., Burr, A., Darque-Ceretti, E., Felder, E., Sbirrazzuoli, N., 2011. Green material composites from renewable resources: polymorphic transitions and phase diagram of beeswax/rosin resin. Thermochim. Acta 521 (1–2), 90–97. https://doi.org/10.1016/j.tca.2011.04.010.

Gao, Y., Lei, Y., Wu, Y., Liang, H., Li, J., Pei, Y., Li, Y., Li, B., Luo, X., Liu, S., 2021. Beeswax: a potential self-emulsifying agent for the construction of thermal-sensitive food W/O emulsion. Food Chem. 349, 129203. https://doi.org/10.1016/j.foodchem.2021.129203.

Geng, Q., Hu, T., Chen, J., Li, C., Li, T., He, X., Han, J., Liu, C., Dai, T., 2024. Emulsion stability enhancement against storage and environment stresses using complex plant protein and betanin. Food Biosci. 59, 104075. https://doi.org/10.1016/j.fbio.2024.104075.

Ghosh, S., Tran, T., Rousseau, D., 2011. Comparison of Pickering and network stabilization in water-in-oil emulsions. Langmuir 27 (11), 6589–6597. https://doi.org/10.1021/la200065y.

Gu, X., Du, L., Meng, Z., 2023. Comparative study of natural wax-based W/O emulsion gels: microstructure and macroscopic properties. Food Res. Int. 165, 112509. https://doi.org/10.1016/j.foodres.2023.112509.

Han, W., Chai, X., Liu, Y., Xu, Y., Tan, C.P., 2022. Crystal network structure and stability of beeswax-based oleogels with different polyunsaturated fatty acid oils. Food Chem. 381, 131745. https://doi.org/10.1016/j.foodchem.2021.131745.

Han, Z., Cheng, K., Pan, Y., Chen, F., Shao, J.H., Liu, S., Sun, Q., Wei, S., Ji, H., 2024. Influence of beeswax-based fish oil oleogels on the mechanism of water and oil retention in Pacific white shrimp (Litopenaeus vannamei) meat emulsion gels: filling, emulsification and phase transition. Food Chem. 458, 140188. https://doi.org/10.1016/j.foodchem.2024.140188.

Hong, X., Zhao, Q., Chen, J., Ye, T., Fan, L., Li, J., 2022. Fabrication and characterization of oleogels and temperature-responsive water-in-oil emulsions based on candelilla (Euphorbia cerifera) wax. Food Chem. 397, 133677. https://doi.org/10.1016/j.foodchem.2022.133677.

Hong, X., Zhao, Q., Liu, Y., Li, J., 2023. Recent advances on food-grade water-in-oil emulsions: instability mechanism, fabrication, characterization, application, and research trends. Crit. Rev. Food Sci. Nutr. 63 (10), 1406–1436. https://doi.org/10.1080/10408398.2021.1964063.

Huang, Z., Guo, B., Gong, D., Zhang, G., 2023. Oleogel-structured emulsions: a review of formation, physicochemical properties and applications. Food Chem. 404, 134553. https://doi.org/10.1016/j.foodchem.2022.134553.

Jana, S., Martini, S., 2014. Effect of high-intensity ultrasound and cooling rate on the crystallization behavior of beeswax in edible oils. J. Agric. Food Chem. 62 (41), 10192–10202. https://doi.org/10.1021/jf503393h.

Jia, G., Zhang, H., 2024. Control of emulsion crystal growth in low-temperature environments. Adv. Colloid Interface Sci. 334, 103313. https://doi.org/10.1016/j.cis.2024.103313.

Kim, Y., Hwang, J.P., Choi, S., Choi, S., Lee, E., Kwon, S.S., Kim, T.H., Cho, Y.J., Kim, K., 2025. Comparison of structural and mechanical properties between water-in-oil high internal phase pickering emulsions stabilized with surface-modified spindle-shaped and amorphous TiO2 particles. Colloids Surf. A Physicochem. Eng. Asp. 707, 135940. https://doi.org/10.1016/j.colsurfa.2024.135940.

Koroleva, M.Y., Yurtov, E.V., 2022. Pickering emulsions: structure, properties and the use as colloidosomes and stimuli-sensitive emulsions. Russ. Chem. Rev. 91 (5), RCR5024. https://doi.org/10.1070/rcr5024.

Liu, C., Zheng, Z., Meng, Z., Chai, X., Cao, C., Liu, Y., 2019. Beeswax and carnauba wax modulate the crystallization behavior of palm kernel stearin. LWT 115, 108446. https://doi.org/10.1016/j.lwt.2019.108446.

Lu, Y., Zhang, R., Jia, Y., Gao, Y., Mao, L., 2023. Effects of nanoparticle types and internal phase content on the properties of W/O emulsions based on dual stabilization mechanism. Food Hydrocoll. 139, 108563. https://doi.org/10.1016/j.foodhyd.2023.108563.

Merchan Sandoval, J., Carelli, A., Palla, C., Baumler, E., 2020. Preparation and characterization of oleogel emulsions: a comparative study between the use of recovered and commercial sunflower waxes as structuring agent. J. Food Sci. 85 (9), 2866–2878. https://doi.org/10.1111/1750-3841.15361.

Metilli, L., Lazidis, A., Francis, M., Marty-Terrade, S., Ray, J., Simone, E., 2021. The effect of crystallization conditions on the structural properties of oleofoams made of cocoa butter crystals and high oleic sunflower oil. Cryst. Growth Des. 21 (3), 1562–1575. https://doi.org/10.1021/acs.cgd.0c01361.

Ming, L., Wu, H., Liu, A., Naeem, A., Dong, Z., Fan, Q., Zhang, G., Liu, H., Li, Z., 2023. Evolution and critical roles of particle properties in Pickering emulsion: a review. J. Mol. Liq. 388, 122775. https://doi.org/10.1016/j.molliq.2023.122775.

Moghtadaei, M., Soltanizadeh, N., Goli, S.A.H., 2018. Production of sesame oil oleogels based on beeswax and application as partial substitutes of animal fat in beef burger. Food Res. Int. 108, 368–377. https://doi.org/10.1016/j.foodres.2018.03.051.

Öğütcü, M., Arifoğlu, N., Yılmaz, E., 2015. Preparation and characterization of virgin olive oil-beeswax oleogel emulsion products. J. Am. Oil Chem. Soc. 92 (4), 459–471. https://doi.org/10.1007/s11746-015-2615-6.

Penagos, I.A., Murillo Moreno, J.S., Dewettinck, K., Van Bockstaele, F., 2023. Carnauba wax and beeswax as structuring agents for water-in-oleogel emulsions without added emulsifiers. Foods 12 (9), 1850. https://doi.org/10.3390/foods12091850.

Qiu, H., Zhang, H., Eun, J.-B., 2024. Oleogel classification, physicochemical characterization methods, and typical cases of application in food: a review. Food Sci. Biotechnol. 33 (6), 1273–1293. https://doi.org/10.1007/s10068-023-01501-z.

Sarkar, A., Dickinson, E., 2020. Sustainable food-grade Pickering emulsions stabilized by plant-based particles. Curr. Opin. Colloid Interface Sci. 49, 69–81. https://doi.org/10.1016/j.cocis.2020.04.004.

Sarkar, A., Zhang, S., Holmes, M., Ettelaie, R., 2019. Colloidal aspects of digestion of Pickering emulsions: experiments and theoretical models of lipid digestion kinetics. Adv. Colloid Interface Sci. 263, 195–211. https://doi.org/10.1016/j.cis.2018.10.002.

Sarkisyan, V., Frolova, Y., Sobolev, R., Kochetkova, A., 2023. On the role of beeswax components in the regulation of sunflower oil oleogel properties. Food Biophys. 18 (2), 262–272. https://doi.org/10.1007/s11483-022-09769-0.

Schaeffer, C., Schummer, C., Scholer, S., van Nieuwenhuyse, A., Pincemaille, J., 2024. Evaluation of environmental contamination in beeswax products. J. Chromatogr. B 1244, 124243. https://doi.org/10.1016/j.jchromb.2024.124243.

Schoening, F.R.L., 1980. The X-ray diffraction pattern and deformation texture of beeswax. South Afr. J. Sci. 76, 262–265.

Septiyanti, M., Fauziyah, N., Harmami, S., Agustian, E., Meliana, Y., 2021. Effect of water content on water in oil (w/o) emulsion properties based on cocoa butter for cosmetic raw material. ARPN J. Eng. Appl. Sci. 16 (22), 2330–2337.

Shi, Z., Wu, J., Wang, X., Nie, T., Zeng, Q., Yuan, C., Jin, R., 2024. Development of Pickering water-in-oil emulsions using a dual stabilization of candelilla wax and acylated EGCG derivatives to enhance the survival of probiotics (Lactobacillus plantarum) powder. Food Funct. 15 (22), 11141–11157. https://doi.org/10.1039/D4FO01342E.

Shu, M., Zhou, Y., Liu, Y., Fan, L., Li, J., 2023. Sucrose esters and beeswax synergize to improve the stability and viscoelasticity of water-in-oil emulsions. Foods 12 (18). https://doi.org/10.3390/foods12183387.

Small, D.M., 1984. Lateral chain packing in lipids and membranes. JLR (J. Lipid Res.) 25 (13), 1490–1500. https://doi.org/10.1016/s0022-2275(20)34422-9.

Song, Y., Zhang, X., Li, J., Zhang, R., Li, B., Li, L., 2025. Surfactant-free W/O high internal phase emulsions co-stabilized by beeswax and phytosterol crystal scaffold: a promising fat mimetic with enhanced mechanical and mouthfeel properties. Food Res. Int. 201, 115614. https://doi.org/10.1016/j.foodres.2024.115614.

Tavernier, I., Doan, C.D., Van de Walle, D., Danthine, S., Rimaux, T., Dewettinck, K., 2017. Sequential crystallization of high and low melting waxes to improve oil structuring in wax-based oleogels. RSC Adv. 7 (20), 12113–12125. https://doi.org/10.1039/c6ra27650d.

Tenorio-Garcia, E., Araiza-Calahorra, A., Rappolt, M., Simone, E., Sarkar, A., 2023. Pickering water-in-oil emulsions stabilized solely by fat crystals. Adv. Mater. Interfac. 10 (31), 2300190. https://doi.org/10.1002/admi.202300190.

Tulloch, A.P., 1971. Beeswax: structure of the esters and their component hydroxy acids and diols. Chem. Phys. Lipids 6 (3), 235–265. https://doi.org/10.1016/0009-3084(71)90063-6.

Wettlaufer, T., Hetzer, B., Flöter, E., 2021. Characterization of oleogels based on waxes and their hydrolyzates. Eur. J. Lipid Sci. Technol. 123 (7), 2000345. https://doi.org/10.1002/ejlt.202000345.

Wijarnprecha, K., de Vries, A., Santiwattana, P., Sonwai, S., Rousseau, D., 2019. Microstructure and rheology of oleogel-stabilized water-in-oil emulsions containing crystal-stabilized droplets as active fillers. LWT 115, 108058. https://doi.org/10.1016/j.lwt.2019.04.059.

Wijarnprecha, K., de Vries, A., Sonwai, S., Rousseau, D., 2021. Water-in-oleogel emulsions—from structure design to functionality. Front. Sustain. Food Syst. 4, 566445. https://doi.org/10.3389/fsufs.2020.566445.

Zhang, Y., Lu, Y., Zhang, R., Gao, Y., Mao, L., 2021. Novel high internal phase emulsions with gelled oil phase: preparation, characterization and stability evaluation. Food Hydrocoll. 121, 106995. https://doi.org/10.1016/j.foodhyd.2021.106995.

Zhang, Y., Wang, Y., Zhang, R., Yu, J., Gao, Y., Mao, L., 2022. Tuning the rheological and tribological properties to simulate oral processing of novel high internal phase oleogel-in-water emulsions. Food Hydrocoll. 131, 107757. https://doi.org/10.1016/j.foodhyd.2022.107757.

Zhang, R., Zhang, Y., Yu, J., Gao, Y., Mao, L., 2023. Enhanced freeze-thawing stability of water-in-oil Pickering emulsions stabilized by ethylcellulose nanoparticles and oleogels. Carbohydr. Polym. 312, 120814. https://doi.org/10.1016/j.carbpol.2023.120814.

Zhao, Q., Jiang, L., Lian, Z., Khoshdel, E., Schumm, S., Huang, J., Zhang, Q., 2019. High internal phase water-in-oil emulsions stabilized by food-grade starch. J. Colloid Interface Sci. 534, 542–548. https://doi.org/10.1016/j.jcis.2018.09.058.